metals

MDPI

Article

In Situ Observation of Crystal Rain and Its Effect on Columnar to Equiaxed Transition

Honggang Zhong [1,2,*], Yunhu Zhang [1], Xiangru Chen [1,*], Congsen Wu [1], Zhiqiang Wei [1] and Qijie Zhai [1,2]

[1] State Key Laboratory of Advanced Special Steel, Shanghai Key Laboratory of Advanced Ferrometallurgy, School of Materials Science and Engineering, Shanghai University, Shanghai 200072, China; yunhuzhang@shu.edu.cn (Y.Z.); qiuxiai@shu.edu.cn (C.W.); ZQW212133@163.com (Z.W.); qjzhai@shu.edu.cn (Q.Z.)

[2] Shanghai Institute of Materials Genome, Shanghai 200444, China

* Correspondence: hgzhong@shu.edu.cn (H.Z.); cxr16@shu.edu.cn (X.C.); Tel.: +86-21-5633-4042 (H.Z.); +86-21-6613-5030 (X.C.)

Academic Editor: Soran Birosca
Received: 30 August 2016; Accepted: 3 November 2016; Published: 8 November 2016

Abstract: The investigation of a columnar to equiaxed transition (CET) and grain refinement is of high commercial importance for the improvement of the solidification structure of metal castings. The crystal rain from the free surface is frequently generated to produce grain refinement and promote a CET in alloys under the application of electromagnetic fields. However, the mechanism underlying the CET influenced by the generated crystal rain is not clear because the employed metallic alloys are opaque. In the present paper, the crystal rain in a transparent NH_4Cl–H_2O solution is produced by blowing a cooled nitrogen gas on the free surface to observe in situ its impact on the occurrence of a CET. The results show that the crystal rain can significantly promote a CET even in a high temperature gradient and that a CET only can occur when the temperature gradient is almost close to zero in the reference experiment. Finally, the most likely mechanism is discussed and clarified.

Keywords: NH_4Cl–H_2O; crystal rain; CET; refinement; physical simulation

1. Introduction

Solidified structures and segregation of castings are of great importance for its mechanical, chemical, and processing properties. Generally, the solidified structure in ingots and billets consists of columnar and equiaxed grains. Columnar grains show anisotropic properties and can induce macrosegregation, whereas fine equiaxed grains can improve the homogeneity of the castings. Hence, the most effective way to improve the homogeneity of ingots and billets is to generate large amounts of equiaxed grains and promote a columnar to equiaxed transition (CET).

According to previous research, the origin of equiaxed grains in ingots is mainly attributed to the free grains detached from the mold walls [1] and the melt surface [2], as well as the nucleation under the constitutional undercooling [3]. Technically, more equiaxed grains can be obtained by adding nucleating agents [4]. However, this chemical method has limitations in many cases. The development of effective nucleation agents in steels has not been very effective yet. Hence, many other methods have been employed to cause grain refinement in solidifying metal alloys, such as electromagnetic stirring (EMS) [5], ultrasonic vibration [6], electric current pulse (ECP) [7,8], pulsed electromagnetic fields [9], and process control methods [10–12]. Recently, Zhai [13] developed a pulse magneto-oscillation (PMO) technique, which could significantly increase the number of free grains and promote a CET in ingots and billets. In particular, the surface pulse magneto-oscillation (SPMO) method [14], putting the electromagnetic coil above the free surface of ingots, can stimulate grain nucleation and detachment

from the surface of liquid metal to cause crystal rain. The crystal rain can block the growth of columnar dendrites and refine the solidification structure significantly. However, the CET mechanism underlying this phenomenon is not clear.

It is unfortunate that the solidification process in metal materials can hardly be observed in situ because they are opaque. Recently, in situ observation of solidifying metals by a synchrotron X-ray technique [15,16] was successfully performed to study the solidification behavior of alloys. However, crystal rain is difficult to generate in a solidification cell because the gap between quartz plates is only 200–300 μm, which can significantly limit the crystal sedimentation and convection in bulk melt. Jackson [17] found several transparent compounds that show similar solidification morphology to metals. Thus, transparent model materials have become ideal simulation materials for the study of the solidification of metals. Peppin [18] observed the steady-state solidification of aqueous ammonium chloride and discussed the effect of the freezing rate and initial concentration of the solution on morphological transitions. Beckermann et al. [19–21] investigated the equiaxed dendritic solidification of a NH_4Cl–H_2O solution with convection. Nayak [22,23] observed and presented numerically the solidification behavior of aqueous ammonium chloride on an inclined cooling plate. Liu [24] observed the detachment of dendrite side arms induced by deceleration in NH_4Cl–H_2O and $[CH_2CN]_2$–H_2O solutions. The effects of vibrational frequency and roughness of the substrate on nucleation were studied using a NH_4Cl–H_2O solution by Wang [25]. Zhang et al. studied the effect of substrate surface structure on the nucleation with NH_4Cl and 70 wt. % H_2O [26,27]. Nonetheless, the effect of crystal rain on the CET has been paid little attention.

In the present paper, the sedimentation of free crystals from the melt surface (crystal rain) was generated and observed in situ in a NH_4Cl–H_2O solution. The influence of the generated crystal rain on the occurrence of a CET was considered, and the related mechanism is herein discussed.

2. Experimental Procedure

A solution of NH_4Cl and 65 wt. % H_2O was selected as the experimental material. Figure 1 shows the setup for the NH_4Cl aqueous solution crystallization. Two quartz tubes (Beijing Zhong Cheng Quartz Glass Co. Ltd., Beijing, China) (open at both ends) with inner diameter of 26 mm and length of 260 mm were used as mold. A cylindrical copper block was inserted into the tube bottom and cooled by an ice water mixture (see Figure 1a). Three K-type thermocouples (Anhui Tian Kang Co. Ltd., Chuzhou, China) were fixed in each mold to measure the temperature evolution, as shown in Figure 1. In order to generate crystal rain in the bulk solution, nitrogen gas was cooled in a spiral copper tube, which was immersed in the ice water mixture, and then directly blown onto the free surface of the solution. As shown in Figure 1c, the cooled nitrogen gas generated a thin solid layer at the free surface and caused certain amounts of free crystals to detach from the solid layer. The gas flux was controlled by a rotameter in a range from 4 L/min to 8 L/min. Since the gas was blown onto the surface of solution, global forced convection was observed inside the bulk solution. A reference experiment was also performed at the same time to show the solidification of a solution of NH_4Cl and 65 wt. % H_2O without the influence of nitrogen gas or crystal rain.

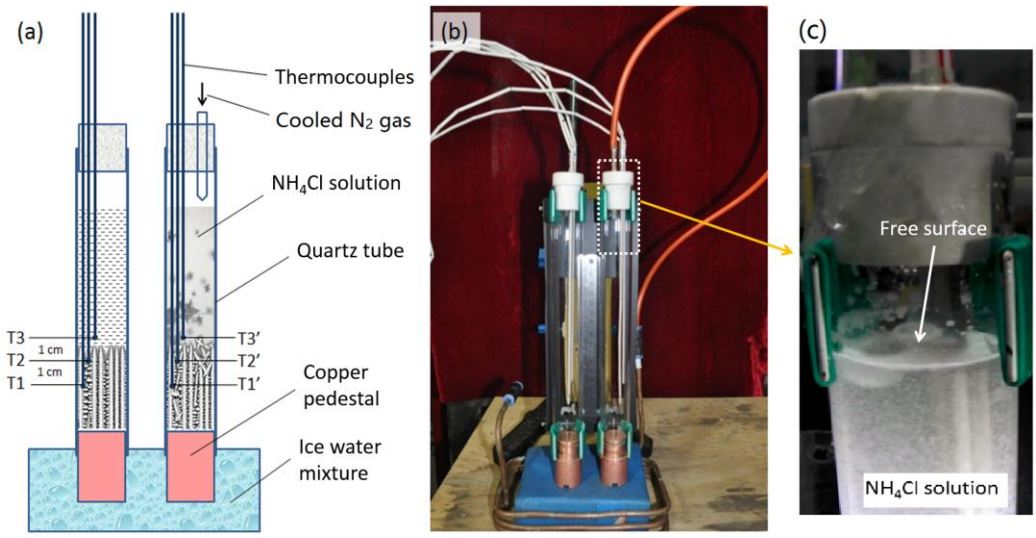

Figure 1. Setup of NH_4Cl aqueous solution crystallization. (**a**) Schematic view; (**b**) device picture; (**c**) picture of free liquid surface and crystals generated by cooled N_2 gas.

The experimental procedure is as follows. The solution of NH_4Cl and 65 wt. % H_2O was heated to 85 °C (or 95 °C, to investigate the effect of superheat on the CET), and it was then poured into the molds to directionally solidify. When the top of the columnar dendrites grew over the bottom thermocouple (T1 and T1′), the cooled nitrogen gas was blown onto the free surface of solution in one of the quartz tubes to cause crystal rain and forced convection inside the bulk solution. The cooling curves were measured via thermocouples. A temperature gradient that divides the temperature difference by the distance difference between the employed thermocouples T2 and T1 (or T2′ and T1′) was defined. The dendritic growth and crystal rain were photographed by a digital single lens reflex camera (Nikon D90) (Nikon Corporation, Tokyo, Japan).

3. Results and Discussion

3.1. Crystal Growth and the CET in the Reference Sample

Figure 2 shows the columnar grains directionally solidified from the bottom of the reference sample, 600 s after the solution was poured into the tube. The coarse columnar dendrite morphology can be observed at the solid–liquid (S–L) interface. It took 750 s for the interface to reach thermocouple T1. In the solidified structure (about 1300 s after pouring), shown in Figure 3, a few small equiaxed crystals (about 0.1 mm in diameter) were clearly observed ahead of the S–L interface as the columnar crystals gradually grew. However, these small equiaxed crystals were not able to stop the growth of columnar crystals and fell into the columnar crystal branches (see in Figure 4, in black dash line circles). When the S–L interface moved over thermocouple T2 (about 1650 s after pouring), numerous larger equiaxed grains formed at the front of the S–L interface to block the growth of columnar crystals. However, no sharp columnar-equiaxed interface was observed, and the CET occurred in a zone (between T2 and T3) where columnar and equiaxed crystals co-exist, which is in agreement with the studies by Ares and Gueijman [28,29]. Generally, there are examples of both kinds of CETs in the literature [30].

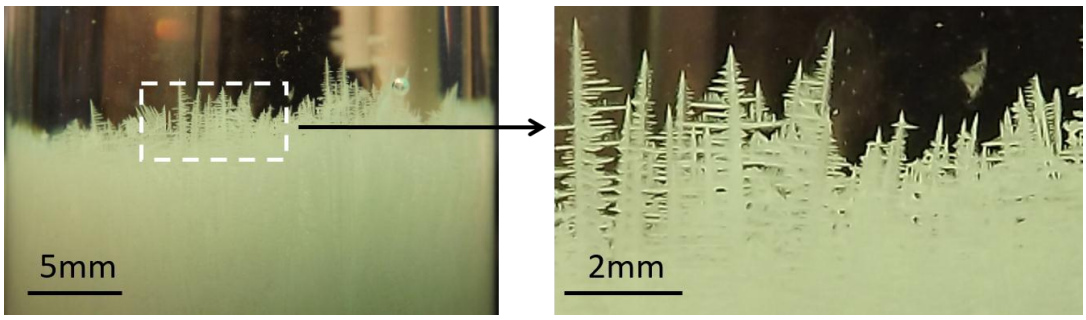

Figure 2. The columnar dendrites of ammonium chloride without the impact of nitrogen gas (600 s after pouring).

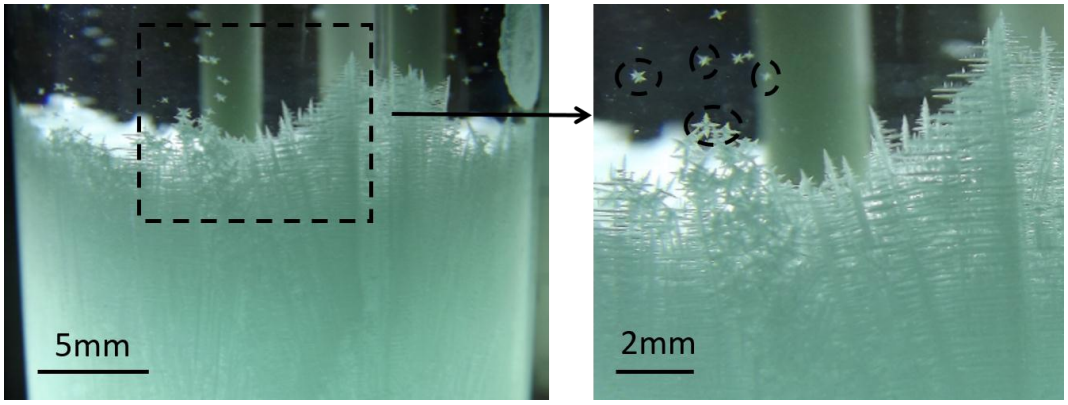

Figure 3. A few equiaxed crystals nucleated in front of the S–L interface and fell in the columnar crystal branches in the reference sample.

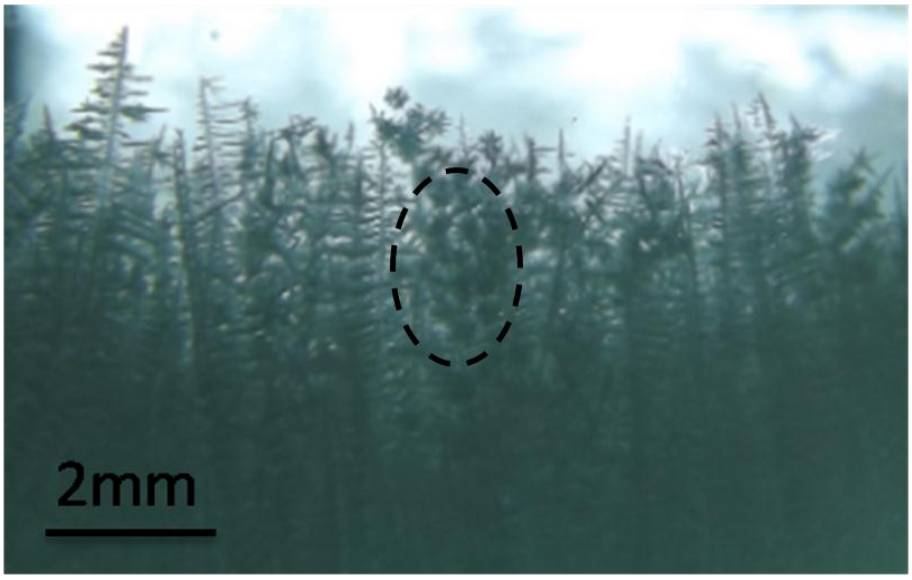

Figure 4. The image of equiaxed crystals falling into the columnar dendritic branches in the reference sample. The equiaxed crystals nucleating in front of the S–L interface are too small in both quantity and size to block the columnar crystals.

3.2. Crystal Rain and Its Effect on the CET

Coarse columnar dendrites with the same growth rate as shown in the reference sample were also achieved in the sample before the nitrogen gas was blown onto the liquid surface. When the S–L interface arrived at thermocouple T1, the cooled nitrogen gas was triggered to cause crystal rain (as shown in Figure 1c). Figure 5 shows the generated crystal rain above the S–L interface in the samples for different nitrogen gas fluxes. A large amount of free equiaxed crystals and the agglomeration phenomenon of free crystals (see Figure 5b) can be observed in the samples with different nitrogen gas fluxes rather than in the reference sample. Moreover, it can be found that the amount of free crystals remarkably increased, and their size reduced significantly when the higher gas flux was employed. In addition, the sedimentation rate of free crystals accelerated with increasing gas flux. When the flow rate was 6–8 L/min (see Figure 5c,d), plenty of fine equiaxed crystals fell onto the S–L interface like a snowstorm. The corresponding sedimentation rates of equiaxed crystals adjacent to the zone above the S–L interface were measured, showing a linear correlation to the intensity of nitrogen gas flux, as shown in Figure 6.

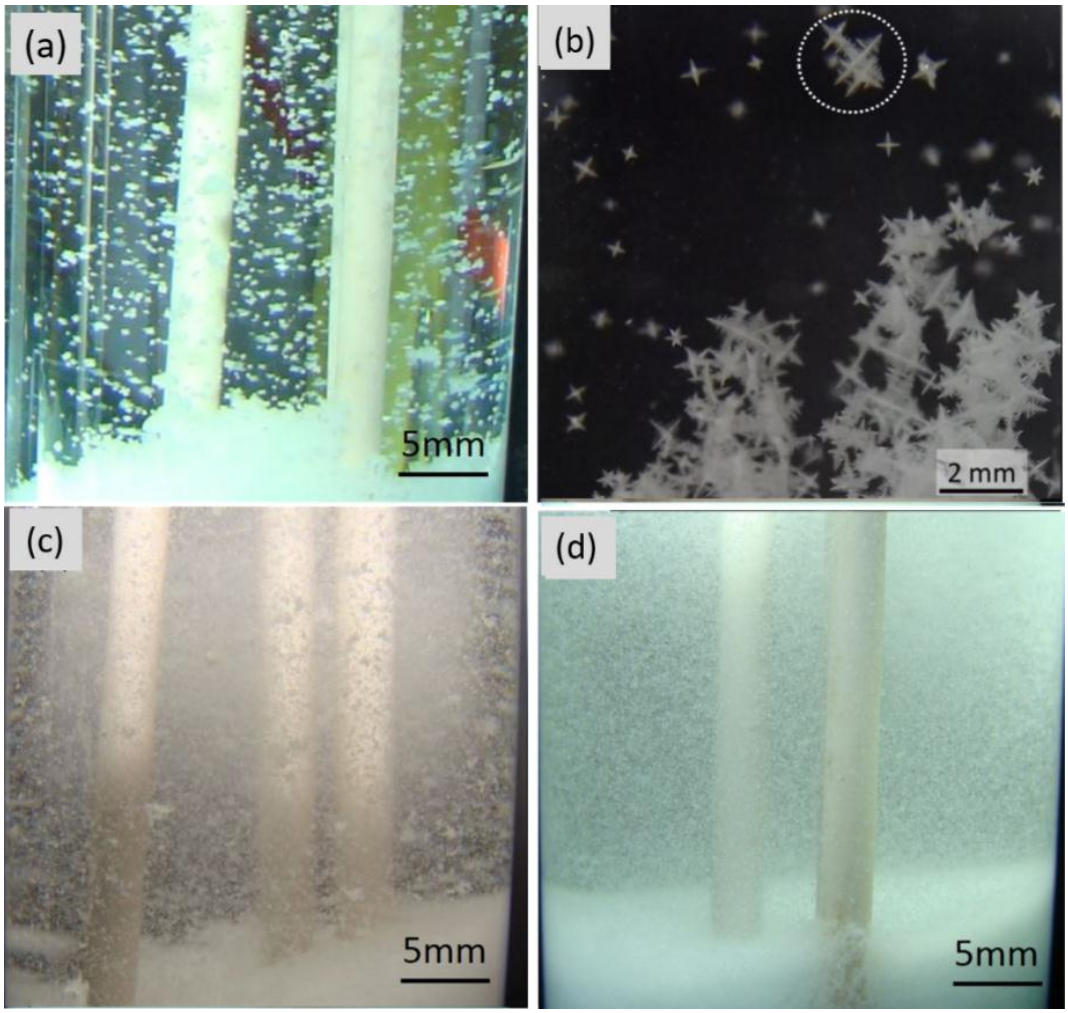

Figure 5. Crystal rain in aqueous solution of ammonium chloride. (**a**) Crystal rain under nitrogen gas flux of 4 L/min; (**b**) some equiaxed crystals agglomerating to each other (nitrogen gas flux = 4 L/min); (**c**) crystal rain under nitrogen gas flux of 6 L/min; (**d**) crystal rain under nitrogen gas flux of 8 L/min.

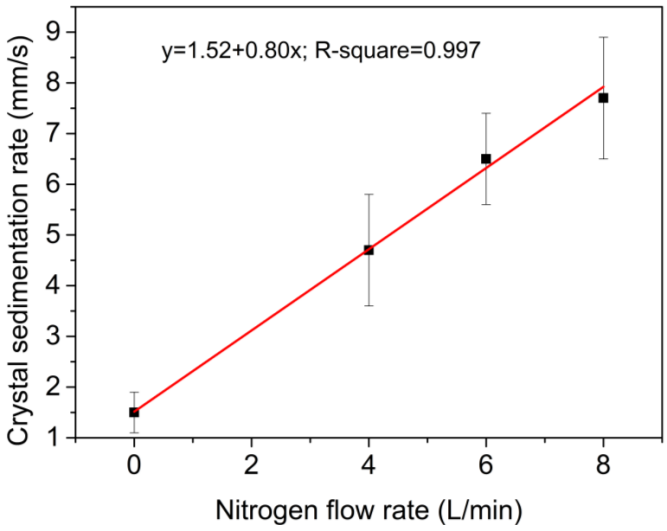

Figure 6. Influence of nitrogen gas flux on the sedimentation rate of equiaxed crystal grains.

Figure 7 shows the measured cooling curves and the corresponding mean temperature gradients accompanying the occurrence of the CET in the samples with and without the influence of the cooled nitrogen gas. The CET in the reference sample occurs in a period after the S–L interface grew over the thermocouple T2. The value of the temperature gradient during the CET period was almost zero—sometimes even negative. This means that the solution just above the S–L interface is undercooled to promote the heterogeneous nucleation of equiaxed grains, which locks the growth of columnar crystals. In comparison with the reference sample, the cooled nitrogen gas causing crystal rain significantly promotes the occurrence of CET. The clear CET interface is formed when the S–L interface grows over the lowest thermocouple T1′. Moreover, it should be noted here that the temperature gradient ahead of the S–L interface is as high as 6 °C/cm when the CET occurs. This indicates that the crystal rain can trigger the CET at one elevated temperature gradient ahead of the S–L interface. In order to confirm this phenomenon, 11 solidification experiments were performed under the application of the cooled nitrogen gas (see Figure 8). The figure shows that the generated crystal rain can still significantly promote a CET, even when the temperature gradient is in the 5–6.5 °C/cm range. Furthermore, it was found that the pouring temperature and the intensity of nitrogen gas flux has no significant influence on the temperature gradient when the CET occurs.

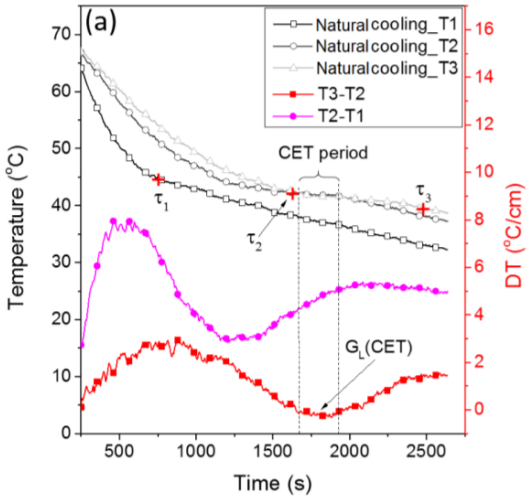

Figure 7. *Cont.*

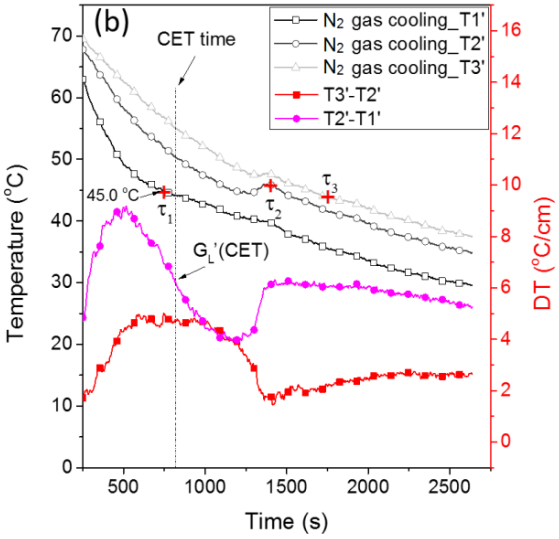

Figure 7. The cooling curves and temperature gradients in the CET zone (pouring temperature: 85 °C, the pouring time is defined as t = 0), (**a**) reference sample; (**b**) sample with crystal rain.

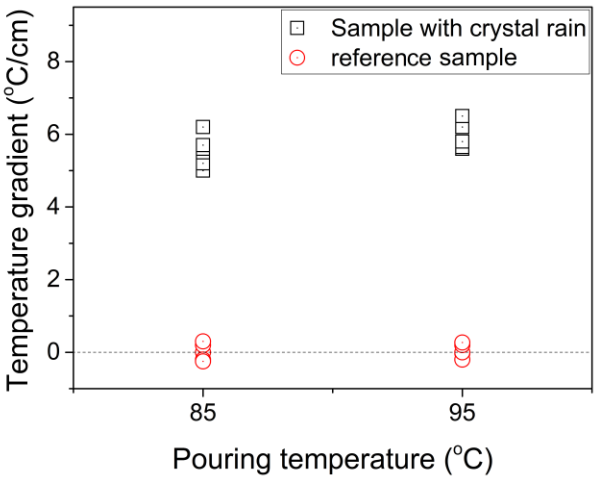

Figure 8. The temperature gradient ahead of the S–L interface during the CET.

3.3. The Mechanism of the CET with Crystal Rain

According to previous investigations, the occurrence of a CET depends on the amount of equiaxed grains, the solute distribution, and the temperature gradient in front of the S–L interface. Nguyen-Thi [31] observed in situ the solute enrichment area surrounding the dendritic microstructure of the Al–Ni alloy. It was found that equiaxed grains appeared in the solute enrichment layer after the pulling rate was increased, and the columnar as well as equiaxed dendrites generally cease to grow long before effective contact, which confirmed that the blocking mechanism in the CET was likely to be solutal [32]. The CET in the reference sample is most likely due to the significant heterogeneous nucleation caused by the constitutional undercooling in the low temperature gradient region.

In case of the sample under the influence of crystal rain, the temperature gradient ahead of the S–L interface was far higher than that in the reference sample when the CET occurs (as shown in Figure 7). It has been shown in the reference sample that few equiaxed grains formed at front of the S–L interface due to the constitutional undercooling when the temperature is about 6 °C/cm. These few nuclei just fell into the columnar dendritic branches and cannot block the growth of columnar grains. In addition, the convection forced by the nitrogen gas flow could reduce the thickness of the

solute-enriched layer and the temperature gradient at the front of the S–L interface [33,34]. Hence, the most likely mechanism of the CET is that the generated crystal rain supplies a sufficient amount of equiaxed crystals to block the growth of columnar crystals.

4. Conclusions

The influence of crystal rain on CET was investigated in situ in a solution of NH_4Cl and 65 wt. % H_2O. The crystal rain can be generated by blowing the cooled nitrogen gas on the free surface of the solution. It was found that nitrogen gas with a higher flux can produce a significantly larger amount of free equiaxed crystals in the bulk solution, and can increase the sedimentation velocity of free crystals at the S–L interface. As a consequence, the CET is immediately provoked by the generated crystal rain, even when the temperature gradient is as high as 6 °C/cm. However, in comparison with the reference experiment, the CET only occurs when the temperature gradient decreases to almost zero. It was deduced that the most likely mechanism underlying the CET promoted by crystal rain is the growth of columnar dendrites mechanically blocked by the generated free equiaxed crystals.

Acknowledgments: The authors acknowledge the financial supports from the NSFC (No. 51227803, 51404150 & 51504148), Science and Technology Commission of Shanghai Municipality (No. 14DZ2261200).

Author Contributions: Honggang Zhong and Qijie Zhai conceived and designed the experiments; Consen Wu performed the experiments and calculation; Yunhu Zhang, Xiangru Chen, Honggang Zhong, and Qijie Zhai analyzed the results and fostered the interpretation; all authors contributed equally to the discussion and writing the paper.

Conflicts of Interest: The authors declare no conflict of interest.

References

1. Ohno, A.; Motegi, T.; Soda, H. Origin of the equiaxed crystals in castings. *Tran. Iron Steel Inst. Jpn.* **1971**, *11*, 18–23.
2. Southin, R.T. Nucleation of the equiaxed zone in cast metals. *Trans. Metall. Soc. AIME* **1967**, *239*, 220–225.
3. Winegard, W.C.; Chalmers, B. Supercooling and dendritic freezing in alloys. *Trans. Am. Soc. Met.* **1954**, *46*, 1214–1224.
4. Sigworth, G.K. The grain refining of aluminum and phase relationships in the Al–Ti–B system. *Metall. Trans. A* **1984**, *15*, 277–282. [CrossRef]
5. Tzavaras, A.A.; Brody, H.D. Electromagnetic stirring and continuous casting—Achievements, problems, and goals. *JOM* **1984**, *36*, 31–37. [CrossRef]
6. Ma, Q.; Ramirez, A.; Das, A. Ultrasonic refinement of magnesium by cavitation: Clarifying the role of wall crystals. *J. Cryst. Growth* **2009**, *311*, 3708–3715.
7. Liao, X.; Zhai, Q.; Luo, J.; Chen, W.; Gong, Y. Refining mechanism of the electric current pulse on the solidification structure of pure aluminum. *Acta Mater.* **2007**, *55*, 3103–3109. [CrossRef]
8. Nakada, M.; Shiohara, Y.; Flemings, M.C. Modification of solidification structures by pulse electric discharging. *Tran. Iron Steel Inst. Jpn.* **1990**, *30*, 27–33. [CrossRef]
9. Kolesnichenko, A.F.; Podoltsev, A.D.; Kucheryavaya, I.N. Action of pulse magnetic field on molten metal. *Tran. Iron Steel Inst. Jpn.* **1994**, *34*, 715–721. [CrossRef]
10. Campbell, J. Grain refinement of solidifying metals by vibration: A review. In Proceedings of the Solidification Technology in the Foundry and Cast House, Proceedings of an International Conference of the Applied Metallurgy & Metals Technology Group, Coventry, UK, 15–17 September 1983; Metals Society: London, UK, 1983; pp. 61–64.
11. Easton, M.A.; Kaufmann, H.; Fragner, W. The effect of chemical grain refinement and low superheat pouring on the structure of NRC castings of aluminium alloy Al–7Si–0.4Mg. *Mater. Sci. Eng. A* **2006**, *420*, 135–143. [CrossRef]
12. Wang, X.; Zhang, H.; Zuo, Y.; Zhao, Z.; Zhu, Q.; Cui, J. Experimental investigation of heat transport and solidification during low frequency electromagnetic hot-top casting of 6063 aluminum alloy. *Mater. Sci. Eng. A* **2008**, *497*, 416–420. [CrossRef]

13. Gong, Y.Y.; Zhai, Q.J.; Li, B.; Li, R.X.; Yin, Z.X. A Method of Refining Solidificaiton Microstructure with Surface Pulsed Magneto-Oscillation. CN Patent 201,010,167,538.3, 5 June 2010.
14. Zhao, J.; Yu, J.; Li, Q.; Zhong, H.; Song, C.; Zhai, Q. Structure of slowly solidified 30Cr2Ni4MoV casting with surface pulsed magneto-oscillation. *Mater. Sci. Technol.* **2015**, *31*, 1589–1594. [CrossRef]
15. Nguyen-Thi, H.; Salvo, L.; Mathiesen, R.H.; Arnberg, L.; Billia, B.; Suery, M.; Reinhart, G. On the interest of synchrotron X-ray imaging for the study of solidification in metallic alloys. *C. R. Phys.* **2012**, *13*, 237–245. [CrossRef]
16. Mathiesen, R.H.; Arnberg, L.; Nguyen-Thi, H.; Billia, B. In Situ X-ray video microscopy as a tool in solidification science. *JOM* **2012**, *64*, 76–82. [CrossRef]
17. Jackson, K.A.; Hunt, J.D. Transparent compounds that freeze like metals. *Acta Metall.* **1965**, *13*, 1212–1215. [CrossRef]
18. Peppin, S.; Huppert, H.E.; Worster, M.G. Steady-state solidification of aqueous ammonium chloride. *J. Fluid Mech.* **2008**, *599*, 465–476. [CrossRef]
19. Beckermann, C.; Wang, C.Y. Equiaxed dendritic solidification with convection. 3. Comparisons with NH_4Cl–H_2O experiments. *Metall. Mater. Trans. A* **1996**, *27*, 2784–2795. [CrossRef]
20. Ramani, A.; Beckermann, C. Dendrite tip growth velocities of settling NH_4Cl equiaxed crystals. *Scr. Mater.* **1997**, *36*, 633–638. [CrossRef]
21. Badillo, A.; Ceynar, D.; Beckermann, C. Growth of equiaxed dendritic crystals settling in an undercooled melt, Part 1: Tip kinetics. *J. Cryst. Growth* **2007**, *309*, 197–215. [CrossRef]
22. Nayak, A.K.; Barman, N.; Chattopadhyay, H. Solidification of a binary solution ($NH_4Cl + H_2O$) on an inclined cooling plate: A parametric study. *Procedia Mater. Sci.* **2014**, *5*, 454–463. [CrossRef]
23. Mohanty, D.; Nayak, A.K.; Barman, N. Studies on transport phenomena during solidification of a binary solution ($NH_4Cl + H_2O$) on an inclined cooling plate. *Trans. Indian Inst. Met.* **2012**, *65*, 801–807. [CrossRef]
24. Liu, S.; Lu, S.; Hellawell, A. Dendritic array growth in the systems NH_4Cl–H_2O and $[CH_2CN]_2$–H_2O: The detachment of dendrite side arms induced by deceleration. *J. Cryst. Growth* **2002**, *234*, 740–750. [CrossRef]
25. Wang, W.; Wang, K.; Lin, X. Crystal nucleation and detachment from a chilling metal surface with vibration. *Mater. Chem. Phys.* **2009**, *117*, 199–203. [CrossRef]
26. Zhang, Y.; Wang, M.; Lin, X.; Huang, W. Effect of substrate surface microstructure on heterogeneous nucleation behavior. *J. Mater. Sci. Technol.* **2012**, *28*, 67–72. [CrossRef]
27. Zhang, Y.; Wang, M.; Lin, X.; Huang, W. Effect of substrate wettability and surface structure on nucleation of crystal. *J. Mater. Sci. Technol.* **2012**, *28*, 859–864. [CrossRef]
28. Ares, A.E.; Gassa, L.M.; Gueijman, S.F.; Schvezov, C.E. Correlation between thermal parameters, structures, dendritic spacing and corrosion behavior of Zn–Al alloys with columnar to equiaxed transition. *J. Cryst. Growth* **2008**, *310*, 1355–1361. [CrossRef]
29. Ares, A.E.; Gueijman, S.F.; Schvezov, C.E. An experimental investigation of the columnar-to-equiaxed grain transition in aluminum-copper hypoeutectic and eutectic alloys. *J. Cryst. Growth* **2010**, *312*, 2154–2170. [CrossRef]
30. Liu, D.R.; Mangelinck-Noël, N.; Gandin, C.A.; Zimmermann, G.; Sturz, L.; Nguyen-Thi, H.; Billia, B. Structures in directionally solidified Al–7 wt.% Si alloys: Benchmark experiments under microgravity. *Acta Mater.* **2014**, *64*, 253–265. [CrossRef]
31. Nguyen-Thi, H.; Reinhart, G.; Mangelinck-NoëL, N.; Jung, H.; Billia, B.; Schenk, T.; Gastaldi, J.; Härtwig, J.; Baruchel, J. In-situ and real-time investigation of columnar-to-equiaxed transition in metallic alloy. *Metall. Mater. Trans. A* **2007**, *38*, 1458–1464. [CrossRef]
32. Martorano, M.; Beckermann, C.; Gandin, C. A solutal interaction mechanism for the columnar-to-equiaxed transition in alloy solidification. *Metall. Mater. Trans. A* **2003**, *34*, 1657–1674. [CrossRef]
33. Willers, B.; Eckert, S.; Michel, U.; Haase, I.; Zouhar, G. The columnar-to-equiaxed transition in Pb–Sn alloys affected by electromagnetically driven convection. *Mater. Sci. Eng. A* **2005**, *402*, 55–65. [CrossRef]
34. Banaszek, J.; Browne, D.J. Modelling columnar dendritic growth into an undercooled metallic melt in the presence of convection. *Mater. Trans.* **2005**, *46*, 1378–1387. [CrossRef]